Driven particle in a one-dimensional periodic potential with feedback control: Efficiency and power optimization

Kiran V.* and Toby Joseph†
Department of Physics, BITS Pilani K K Birla Goa Campus, Zuarinagar 403726, Goa, India

(Received 12 July 2022; accepted 13 October 2022; published 21 November 2022)

A Brownian particle moving in a staircaselike potential with feedback control offers a way to implement Maxwell's demon. An experimental demonstration of such a system using sinusoidal periodic potential carried out by Toyabe *et al.* [Nat. Phys. **6**, 988 (2010)] has shown that information about the particle's position can be converted to useful work. In this paper, we carry out a numerical study of a similar system using Brownian dynamics simulation. A Brownian particle moving in a periodic potential under the action of a constant driving force is made to move against the drive by measuring the position of the particle and effecting feedback control by altering potential. The work is extracted during the potential change and from the movement of the particle against the external drive. These work extractions come at the cost of information gathered during the measurement. Efficiency and work extracted per cycle of this information engine are optimized by varying control parameters as well as feedback protocols. Both these quantities are found to crucially depend on the amplitude of the periodic potential as well as the width of the region over which the particle is searched for during the measurement phase. For the case when potential flip (i.e., changing the phase of the potential by 180°) is used as the feedback mechanism, we argue that the square potential offers a more efficient information-to-work conversion. The control over the numerical parameters and averaging over large number of trial runs allow one to study the nonequilibrium work relations with feedback for this process with precision. It is seen that the generalized integral fluctuation theorem for error-free measurements holds to within the accuracy of the simulation.

DOI: 10.1103/PhysRevE.106.054146

I. INTRODUCTION

The feedback control associated with Maxwell's demon like setups allows one to extract heat from a thermal bath and convert it into useful work [1,2]. In the Szilard engine version of the Maxwell demon implementation, the demon determines whether a single molecule present in a vessel which is in contact with the thermal bath is on the left or right half and uses that information to extract work via isothermal expansion of one of the pistons at the ends of the vessel [3]. The engine apparently seems to violate the second law of thermodynamics. After almost half a century of controversies and discussions, the paradox has been resolved with the understanding (for alternative views, see Refs. [4–8]) that it is possible to extract work from such a system without contradicting the second law of thermodynamics, provided one has accounted for the cost of information processing carried out by the demon [2,9–12]. In another words, it is possible to convert information into free energy or extract work using the available information. Though the problem itself is more than a century old, experiments implementing the demon were only achieved fairly recently both in classical [13–16] and quantum systems [17–22].

One of the first experimental studies of a classical system that converts information into free energy using feedback control was demonstrated by Toyabe *et al.* [13]. In this experiment, a colloidal particle in contact with a thermal bath undergoes rotational Brownian motion in a staircaselike potential with the step height comparable to k_BT. The staircase like potential is created by a combination of a sinusoidal potential and a linear one. The particle can take energy from the thermal bath and make an upward jump or can slide down in the direction of the negative gradient of the potential. In the experiment, one selectively manipulates such fluctuations via position measurement of the particle and subsequent feedback control to extract work from the heat bath. The feedback control was carried out by changing the phase of the sinusoidal potential by 180° (referred to as potential flip), depending on the outcome of the measurement of particle's angular position. The feedback control helps to extract useful work from the thermal bath via two routes: (i) the work done against the linear potential (which the authors refer to as the free-energy gain, ΔF) and (ii) as work extracted during potential flip (referred to as $-W$). The work extracted is accounted for by the energy equivalent of information obtained during the measurement process and there is no violation of the second law. The efficiency of conversion of information to work extracted of the engine is 28%. One of the motivations for the present work is to use simulations to better understand the low efficiency values and explore ways on optimizing this engine.

Many recent works, both in experiments [15,23,24] and in theory [25–27], have looked at ways to improve efficiency and power of information engines. In the domain of classical information engines, the Brownian information engine based

*kiran.vktm@gmail.com, p20180029@goa.bits-pilani.ac.in
†toby@goa.bits-pilani.ac.in

on a colloidal particle in a harmonic potential has been studied extensively [28,29]. But similar detailed study on optimization of the information engine based on particle moving in a periodic potential is lacking. One way to improve the low value of efficiency is by fine tuning the parameters and optimizing the control protocol of the feedback processes. A general feedback scheme for extracting maximum work is by changing the Hamiltonian of the system right after the measurement in such a way that the post measurement state is an equilibrium state of the new Hamiltonian [28,30–33]. Such a protocol is completed by reversibly adjusting the external parameters to the final values. In the present work, we vary the shape of the periodic potential as well as the parameters in the feedback protocol to achieve optimal conversion of information to work based on this principle.

Advances in the area of stochastic thermodynamics in the last few decades have augmented our understanding of how irreversibility emerges from reversible dynamics [34,35]. Various fluctuation theorems have provided insights about entropy production and statistical relationships between work and free energy for systems driven far away from the equilibrium [36–39]. The Jarzynski equality (JE) given by $\langle e^{(\Delta F-W)/k_BT}\rangle = 1$ was one of the first work relations to be derived and it relates the fluctuations in work during a nonequilibrium process to the free-energy difference between the final and initial equilibrium states [38]. This relation breaks down in the presence of feedback process. For processes involving error free measurement and feedback, one can derive a generalized integral fluctuation theorem (GIFT) given by $\langle e^{(\Delta F-W)/k_BT-I+I_u}\rangle = 1$, where I is the information gained during the measurement process and I_u is the unavailable information measured using the time-reversed process (see discussion in Sec. V for details) [40]. The JE itself takes a modified form given by $\langle e^{(\Delta F-W)/k_BT}\rangle = \gamma$, where γ (referred to as efficacy) measures the reversibility of the process. Experimental verification of these relations have been done for a few systems [13,41–43]. The simulations presented here allow for checking the validity of these generalized fluctuation theorems with precision for the studied system.

The paper is organized as follows. The following section introduces the model. In Sec. III, we discuss the details of the simulation and the results. Drift of the particle per cycle and efficiency of information to work conversion for different values of feedback delay are studied. Various optimization studies of efficiency are presented in Sec. IV. These include improvement of efficiency by optimizing the parameters of the model and alteration of feedback protocol. The section ends with the discussion of efficiency of a similar system but with a square potential. In Sec. V, the generalized integral fluctuation relation is discussed and verified for this system and in Sec. VI we summarize and discuss the results.

II. THE MODEL

Consider a particle moving in a sinusoidal potential under the influence of a constant driving force. The net potential in which the particle moves is given by (see Fig. 1)

$$U(x) = \pm U_0 \sin(2\pi x) - F_d x, \tag{1}$$

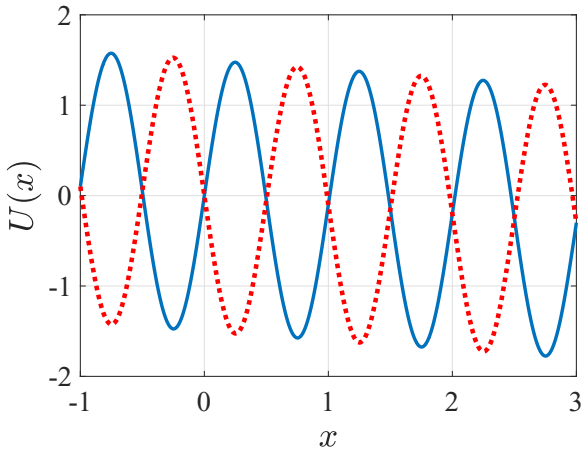

FIG. 1. Tilted sinusoidal potential with period equal to 1 unit. The amplitude of the sinusoidal part and slope corresponding to the uniform force are 1.5 (in units of k_BT) and 0.1 (in units of k_BT per period of the potential), respectively. The red and blue curves correspond to the potential before and after switching of the phase of the sinusoidal part of the potential.

where x is the position of the particle, $2U_0$ gives the depth of the periodic potential, and F_d is the magnitude of the driving force. The $\pm$ sign in the first term in the right-hand side is present because the phase of the potential is changed during the feedback process (see below). Additionally, the particle is in contact with a thermal bath kept at temperature T. The Lagenvin equation governing the motion of the particle is given by

$$m\ddot{x}(t) = -m\xi\dot{x}(t) \pm 2\pi U_0 \cos[2\pi x(t)] + F_d + \zeta(t), \tag{2}$$

where m is the mass of the particle and $-m\xi\dot{x}$ is the viscous force. $\zeta(t)$ is the thermal noise with zero average and the correlation function is given by $\langle\zeta(t)\zeta(t')\rangle = \Gamma\delta(t-t')$. Fluctuation-dissipation relation connects the strength of the noise, Γ, to the friction coefficient, ξ, by the relation: $\Gamma = 2m\xi k_BT$. In the overdamped limit, one can ignore the inertial term in Eq. (2) and this leads to the Brownian dynamics equation,

$$\dot{x} = \frac{\pm 2\pi U_0 \cos(2\pi x) + F_d}{m\xi} + \frac{\zeta}{m\xi}. \tag{3}$$

The feedback process that is designed to help the particle move in the direction opposite to that of the externally applied driving force, $F_d\hat{x}$, and gain free energy in the process is as follows: At times given by $t = n\tau$, a measurement of particle's position is carried out. If the particle is located in the region S (see Fig. 2), then the phase of the potential is changed by π instantaneously (henceforth called potential flip) at a time $t = n\tau + \epsilon$, where ϵ is the feedback delay time. If the particle is not spotted in the region S, then no feedback process is initiated. We shall later alter this feedback procedure in order to improve information to free-energy conversion efficiency. These alterations would involve, in addition to the potential flips, the raising of the potential barrier when the particle is not spotted in S.

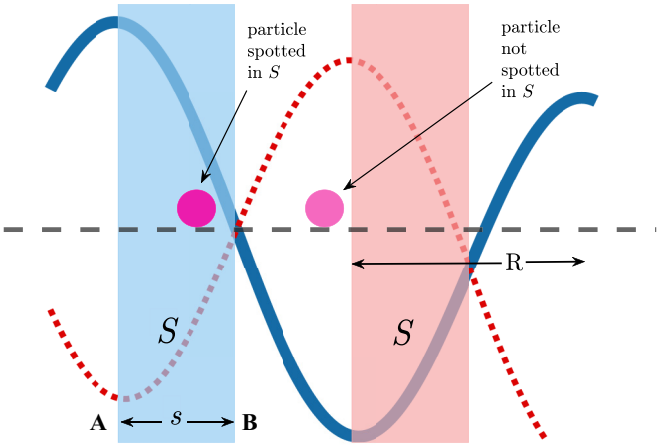

FIG. 2. For measurements carried out at time $t = n\tau$, the particle can be either spotted in region S or outside of S. The feedback protocol is initiated according to the outcome of the measurement. The sinusoidal potential is flipped with a time delay of ϵ, if the particle is spotted in S. The solid blue and dashed red curves correspond to the potential before and after the flip. The S regions are indicated for both the potential configurations before and after flip, with the colors respect to the sinusoidal curves. s is the width of the region S. R is the region to the right of the potential minimum.

III. RESULTS FROM THE SIMULATION

The over-damped equation of motion, Eq. (3), has been integrated numerically using the discretized version [44],

$$x(t+\delta t) = x(t) + \frac{\pm 2\pi U_0 \cos(2\pi x) + F_d}{m\xi}\delta t + f_g, \qquad (4)$$

where δt is the time step and f_g is a Gaussian distributed random variable with zero mean and variance equal to $\frac{2k_BT}{m\xi}\delta t$. We work with a system of units defined by $\xi = 1$, $m = 1$, and $k_BT = 1$. Length scale in the problem is set by the period of the potential, which is 1 and the timescale is ξ^{-1}, which is also 1. The integration time step of the simulation is taken to be $\delta t = 0.0001$ and has been checked for convergence by carrying out simulations at one order less than this value. For the results quoted in this section, the amplitude of the sinusoidal potential is taken to be $U_0 = 1.5$ and the magnitude of the driving force is $F_d = 0.1$. All the feedback processes in our study involve a single cycle and the duration of the cycle is $\tau = 0.05$. Before each cycle starts, we ensure that a long enough equilibration run is carried out so that correlation effects do not affect the results. The region S starts from the maxima of the potential (point A in Fig. 2) and ends at the point where the force is maximum (point B in Fig. 2), encompassing a total length of $s = 0.25$. The feedback delay time, ϵ is varied from the minimum value possible of 0.0001 (since $\delta t = 0.0001$) to 0.047. The mean values of various quantities of interest are determined by averaging over 10^6 cycles.

A. Particle drift and efficiency

The physical quantities of relevance to study the stochastic thermodynamics of the system are (i) the drift velocity of the particle (which is related to the rate at which the system gains free energy), (ii) the work done by the external agent in flipping the potential, and (iii) the information gained during the measurement. The average drift velocity of the particle is given by

$$v_d = \frac{\langle D\rangle}{\tau}, \qquad (5)$$

where $D = x(\tau) - x(0)$ is the distance between the initial and final equilibrium locations of the particle. The angular brackets indicate average over the trials. Note that in the absence of the feedback process, the particle will drift in the direction of the drive and the average speed in the steady state can be exactly evaluated [45,46]. But with feedback, the drift in the direction of drive can be reduced and even reversed, depending on how effective the feedback process is. The free energy gained per cycle, which is the work done against the external force in one cycle, is given by

$$\Delta F = -F_d D, \qquad (6)$$

which is positive if the particle has drifted against the direction of the drive. The work done by the external agent is given by change in the potential energy of the particle in the sinusoidal field at the instant the potential flip is carried out. That is,

$$W = \pm 2\cos[2\pi x(\epsilon)], \qquad (7)$$

where the + sign is for the case when the potential after the flip is greater than its value before the flip, implying that the work is done by the external agent. If otherwise, then the work is being extracted out of the heat bath. The work done in a given cycle is zero if the particle is not spotted in the region S (as there is no potential flip carried out in this case).

The measurement carried out at the beginning of a cycle gives information about the location of the particle and is quantified by the Shannon information content, defined as $\langle I\rangle = -p\ln p - (1-p)\ln(1-p)$ [47] where p is the probability for finding the particle in the region S. The energy equivalent of information content is $k_BT\langle I\rangle$. For the values of s, U_0, and F_d used in the results in this section, the value of $k_BT\langle I\rangle = 0.24$. In the measurement process, an amount of heat equal to $k_BT\langle I\rangle$ is dissipated to the heat bath. This dissipation is associated with the erasure of memory bits required for the measurement. The feedback process allows one to regain a part of this dissipated energy back in the form of an increase in free energy of the particle and also possibly as work extracted from the heat bath. But this regain is possible provided the information obtained is used before the particle equilibrates after the measurement.

The efficiency of the information engine can be defined as

$$\eta = \frac{\langle \Delta F - W\rangle}{k_BT\langle I\rangle}, \qquad (8)$$

which is a measure of how efficiently the available information is converted to free-energy gain and work extracted. ΔF is the change in free energy and $-W$ is the work extracted, as defined above. Variation of efficiency and drift per cycle of the particle for different values of feedback delay ϵ are shown in Figs. 3 and 4, respectively. The efficiency is maximum for minimal feedback delay and maximum value of efficiency is around 41% for a feedback delay of 0.0001. The inset of Fig. 3 shows the individual variation of ΔF and $-\langle W\rangle$ with ϵ. For low values of ϵ, the contribution of $-W$ to the total

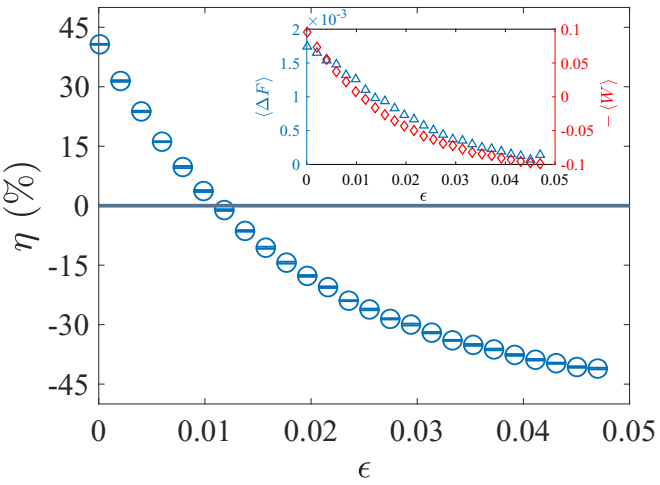

FIG. 3. Variation of efficiency with feedback delay time. For $\epsilon \lesssim 0.01$ (measured in units of $1/\xi$) the system works as an information engine converting information to work. For larger values of ϵ, the efficiency becomes negative indicating that sum of gain in free energy and work extracted is negative. The maximum value of efficiency obtained is 41% at $\epsilon = 0.0001$. The inset shows the contributions of ΔF and $-\langle W \rangle$ separately. For low values of ϵ, $-\langle W \rangle$ term is positive and one order larger than the ΔF. For large values of ϵ, $-\langle W \rangle$ becomes negative implying that work has to be done by the external agent. The error bars in the main figure are standard deviations.

work extracted is much greater than that of ΔF. The system is not working as an information engine for large values of ϵ (the region where $\eta < 0$). In this regime $\langle \Delta F - W \rangle$ is negative and heat is dissipated into the heat bath during the cycle. This is over and above the amount $k_B T \langle I \rangle$ that needs to be dissipated for memory erasures associated with acquiring positional information during the measurement phase.

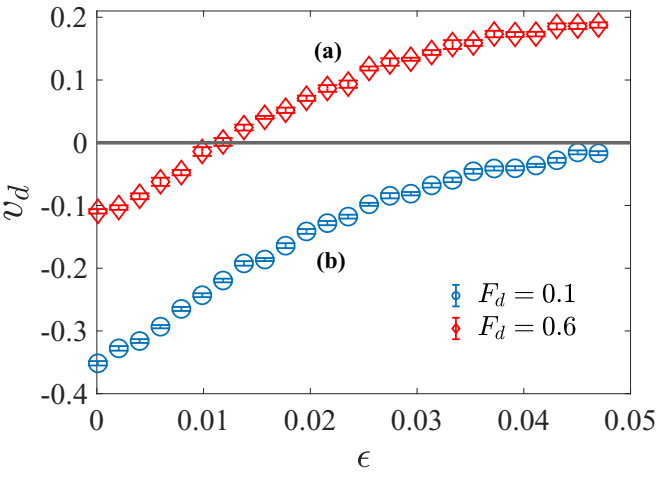

FIG. 4. Variation of particle's velocity (measured in units of period of potential times ξ) as a function of feedback delay time, ϵ. Negative value of displacement indicates net drift in the direction opposite to the uniform external force. For large values of ϵ, the effect of feedback is reduced progressively. The (a) and (b) data points correspond to two different external drives, $F_d = 0.6$ and $F_d = 0.1$, respectively. The error bars in the figure are standard deviations.

The monotonic decrease of the efficiency with increasing feedback delay can be understood as follows. Let us consider the situation that the particle is spotted in S when the measurement is carried out at time $t = 0$. For small values of feedback delay, ϵ, the particle has a significant chance to stay close to the current location (in S) by the time potential flip is carried out. As a result, the particle loses potential energy during the potential flip. This means that work is done by the system (W is negative) [refer to Eq. (7)]. Additionally, for small ϵ value, there will be a net drift toward the left on the average, as seen in Fig. 4 (circles). This is because the particle will be spotted in S only when it makes a leftward jump (against the applied force) with respect to its current equilibrium position and instantly switching the potential phase locally traps the particle in the new minima to the left. This helps the particle to move against the driving force direction which in turn results in a positive free-energy change (since the displacement D of the particle will be negative). Both of these reasons lead to a larger efficiency value for small feedback delays, for a given amount of information obtained. However for large values of ϵ, the particle will most likely move to the right after it is spotted in S, because of the net force in that direction and will equilibrate in one of the minima of the potential. Consequently, the external agent has to do work (W is positive) on the particle during potential flip, since the potential energy of the particle after the flip is likely to be larger). Also, the particle is more likely to move toward the right after the potential flip as there is a slight bias in the steady-state distribution of the particle to the right due to the applied uniform force. This leads to a decrease in the free energy on the average.

It is seen that even for low values feedback delay time, the efficiency of the information to free-energy conversion is very less (≈40%). One reason for the low value of efficiency is the fact that there is no feedback implemented when the particle is not found in S during the measurement. This means, one is not utilizing the full available information for feedback control. For the parameters used in above simulations, value of $p = 0.067$ and the corresponding value of $\langle I \rangle = 0.24$. If we do not provide feedback when the particle is not found in S, the maximum information that we can hope to convert to free energy or work is $-p \ln p = 0.18$. This is about 75% of the total information gathered and so the unused information cannot fully account for the low value of efficiency seen. The primary reason for low efficiency is due to the fact that the feedback process is not reversible in the sense that the time-reversed protocol do not lead to time-reversed processes [30] and thus the engine is working suboptimally. One can modify the protocols to try and optimize the information to free-energy conversion. We discuss these below.

IV. OPTIMIZATION STUDIES

In this section we address the following question: Given a fixed external drive ($F_d = 0.1$, in our studies), how can one optimize the conversion of information to free energy? To start with, we fix the shape of the external potential to be sinusoidal and vary the parameters s and U_0 sequentially to search for maximum efficiency. This achieves only a partial optimization as we are not scanning the entire parameter space. The intention is to see the scale of dependence of

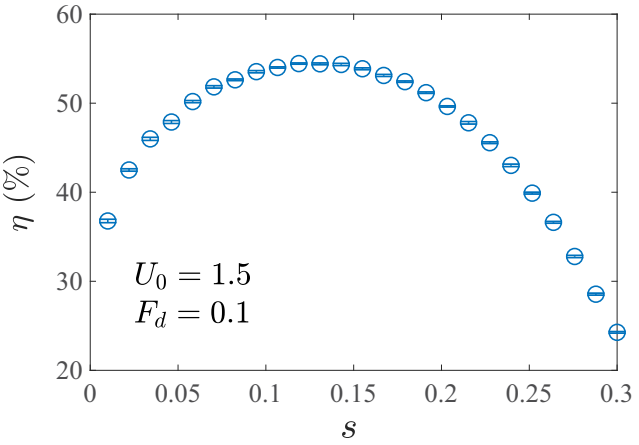

FIG. 5. Optimization of efficiency with respect to parameter s. For the values of $U_0 = 1.5$ and $F_d = 0.1$, a maximum efficiency value of 54.4% is obtained for $s = 0.12$. The error bars in the figure are standard deviations.

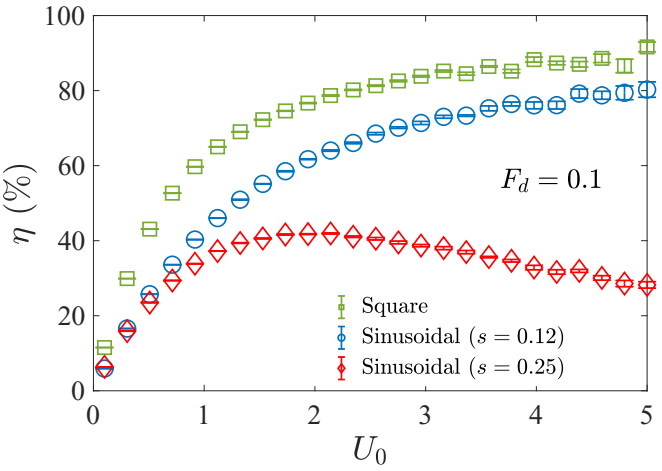

FIG. 6. Variation of efficiency with the amplitude for $s = 0.12$ (blue circles) and $s = 0.25$ (red diamonds). The maximum value of efficiency for $s = 0.12$ is about 80%. We have also shown the dependence of η on amplitude of the potential for the square shaped potential (green squares) with region S' (shown in the inset of Fig. 9 in Sec. IV C) as the searched region during measurement. The maximum efficiency for this case is close to 90%. The error bars in the figure are standard deviations.

efficiency on these parameters. Next, we alter the feedback by associating a protocol when the particle is not spotted in the region S during particle's position measurement, which enables more use of the available information for work extraction. We end the optimization studies by finding efficiency of the system by using square potential instead of a sinusoidal shaped one. We shall argue that the square potential increases the reversibility of the feedback process, leading to larger values of engine efficiency.

A. Parameter optimization for sinusoidal potential

The partial optimization with respect to experimental parameters was done as follows: First we find the optimum value of s for which we get a maximum efficiency by keeping the values of U_0 and F_d fixed at 1.5 and 0.1, respectively. s is varied by keeping the location of the starting point of region S fixed at the maxima of the potential. Efficiency is seen to have nonmonotonic variation with s and the maximum is found to be at $s = 0.12$ as shown in the Fig. 5. The nature of variation of efficiency with s can be understood as follows. For $F_d = 0.1$, the value of ΔF is negligible compared to the work extracted, $-W$. Therefore the major contribution to $\Delta F - W$ comes from work extracted during the potential flip. The work done is $W \approx -2U_0 p(s)$, when the S is a narrow region lying close to the maxima of the potential. Thus for low values of s, we have $\eta(s) = 2U_0 p(s)/\langle I(p(s))\rangle$, which decreases as p decreases. Since p decreases with s, the downward trend of efficiency for small s values is expected. At large values of s, an increase in s leads to a decrease in $-W$ as the particle is more likely to be spotted in regions where the potential flip will lead to less work extraction. Given that $\langle I\rangle$ is an increasing function of s (when $p < 0.5$), it is expected that the efficiency decreases with s for large s values. The maximum value obtained for η is 54.4%, which is 33% more efficiency than for the s value used in the previous section and also in the experimental study [13]. Optimization of efficiency with respect to amplitude U_0 is done by keeping the value of $s = 0.12$, obtained above. As seen from Fig. 6, efficiency increases with amplitude and attains a maximum value of about 80% for amplitude $U_0 \gtrapprox 4.0$. The increase in efficiency with amplitude can be understood as follows: As U_0 increases the energy equivalent of available information, $k_B T\langle I\rangle$ decreases because the probability to find the particle in region S decreases. The average work extracted during the flip ($\langle -W\rangle$) has a more complex dependence on U_0. The work done during individual flip of the potential will increase with U_0 on the average, but the occurrence of flips itself become exponentially less likely with increasing U_0. This leads to the behavior seen where $-W$ increases initially with U_0 but then falls to zero very fast as can be seen in Fig. 7. For low values of U_0 (compared to $k_B T$) the efficiency tends to zero since $-W$ is negligible and $k_B T\langle I\rangle$ is finite. At large values of U_0, both the numerator and denominator in the expression for efficiency tend to zero, leading to a relatively flat curve.

Even though there is a substantial increase in the efficiency attained by increasing the U_0 value, it comes with the cost of extremely low value for work extracted per cycle of the information engine. The low values of p at large U_0 make the available information limited. The dependence of work extracted per cycle on the amplitude is show in Fig. 7. We have also shown in the same figure the behavior of work extracted per cycle with amplitude for $s = 0.25$. In fact, $s = 0.25$ gives better values for this quantity than the efficiency optimized parameter value of $s = 0.12$. In both cases, the maximum value of work per cycle is obtained for a potential amplitude of $U_0 \approx 0.9$, which is of the order of $k_B T$. The maximum value of work per cycle for optimized and nonoptimized case are correspondingly 0.07 and 0.12 in relevant units.

B. Feedback protocol studies

As pointed out at the end of Sec. III, one of the reasons for the protocol used to be suboptimal is that there is no

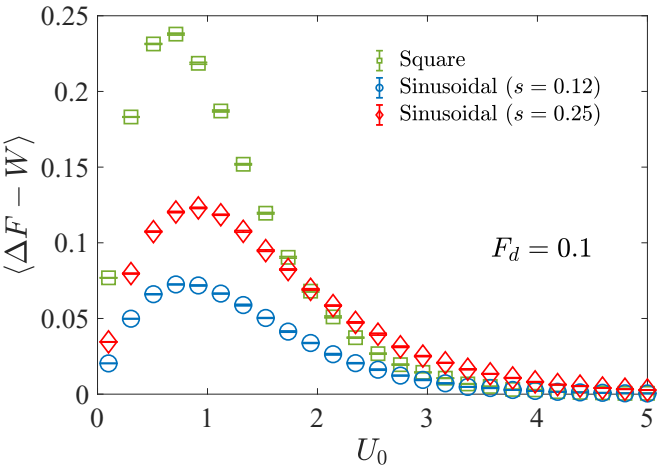

FIG. 7. Variation of total work extracted per cycle with amplitude of potential for $s = 0.12$ (blue circles) and for $s = 0.25$ (red diamonds). The functions have peaks close to $U_0 = 0.9$. Work extracted per cycle is more with $s = 0.25$. The work extracted per cycle as a function of U_0 for the case of square potential with S' region as the search location during measurement (green squares) shows a much more prominent peak. The value location of the peak is marginally lower at $U_0 \approx 0.7$. The error bars in the figure are standard deviations.

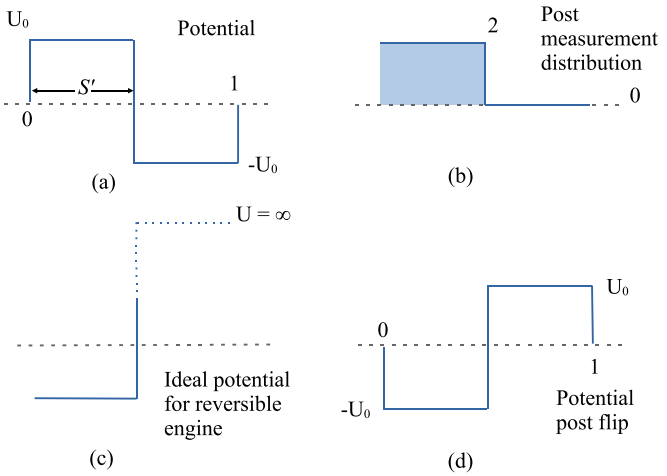

FIG. 8. Feedback process with square periodic potential. (a) The initial shape of the potential energy function. S' is the region where particle is probed for during the measurement. (b) Post measurement distribution of the particle for the case when particle is spotted in the region S'. (c) The potential that has its equilibrium distribution as the post measurement distribution for the case when the particle is spotted in S'. (d) The flipped potential at the end of the cycle.

feedback employed when the particle is *not* spotted in S. By incorporating a feedback protocol for the negative result of the measurement outcome, we can improve the efficiency of the engine. One way to do this would be by raising the potential barrier height (deepening the well) when the particle is not spotted in S. This would increase the efficiency by mitigating the motion of particle in the direction of the drive. When the particle is not spotted in S, the chance that the particle is to the right of the potential minima (region R in Fig. 2) is more than it is otherwise. So by raising the amplitude of the potential, the possibility of the particle drifting in the direction of of the external drive is reduced, thus helping in cutting the loss of free energy.

We have implemented this protocol with the parameters values kept same as in Sec. III. In the new protocol, in addition to the potential flip carried out when the particle is seen in S, the amplitude of the potential is increased from U_0 to $1.1U_0$, when it is not. The increased value of amplitude is maintained until $t = 0.0490$ and the potential amplitude is reverted to its original value at the end of the cycle at $t = \tau(0.05)$. Such a modification in the feedback protocol increased the efficiency marginally from around 41% to about 43%. It is seen that the new protocol could marginally reduce the movement of the particle in the direction of drive. The gain in efficiency is not appreciable due to the fact that the changes in ΔF is not very crucial for the total work extracted, since the key contribution is coming from the $-W$ term.

C. Square potential

We can extract maximum work using feedback by instantaneously changing the Hamiltonian of the system after the measurement such that the post measurement state of the system is identical to the equilibrium state of the new Hamiltonian [30,32]. Such a protocol avoids dissipation as the particle density does not have to relax to the new equilibrium distribution. If one now changes the potential back to its original form quasistatically, then one can extract maximum work in the full cyclic process. In a scheme where the measurement amounts to finding the presence of the particle within a region and feedback protocol employs flipping of the potential, the choice of a square potential would come closest to achieving the above condition. This can be justified as follows: Consider a square of period one given by

$$\begin{aligned} U_s(x) &= U_0 \quad (0 < x \leqslant 0.5) \\ &= -U_0 \quad (0.5 < x \leqslant 1), \end{aligned} \tag{9}$$

with $U_s(x) = U_s(x+1)$ [see Fig. 8(a)]. Consider S' to be the region between between $x = 0$ and $x = 0.5$ where the particle is searched for in the measurement phase. The post measurement density when the particle is spotted in S' has a uniform value equals to 2 in region S' and zero outside of S' [see Fig. 8(b)]. To implement the reversible scheme, one would then have to switch the potential to an infinite barrier shape as shown in Fig. 8(c) and then quasistatically bring it back to the flipped potential shown in Fig. 8(d). Since we are restricting ourselves to potential flips, we bypass the intermediate step. For large barrier height compared to k_BT, the loss incurred in this bye-passing of the intermediate procedure will be minimal because post measurement density distribution will then be very close to the equilibrium distribution for the flipped potential.

We have carried out the simulations by replacing the sinusoidal potential with an approximate form for square potential, obtained by keeping the first 10 terms in the Fourier series expansion of a periodic square potential of amplitude U_0. That is, $U(x) = \frac{4U_0}{\pi} \sum_{n=1(\text{odd})}^{19} \frac{1}{n} \sin(2n\pi x)$. The uniform external drive is kept the same as before. The resultant net potential is shown in the inset of Fig. 9.

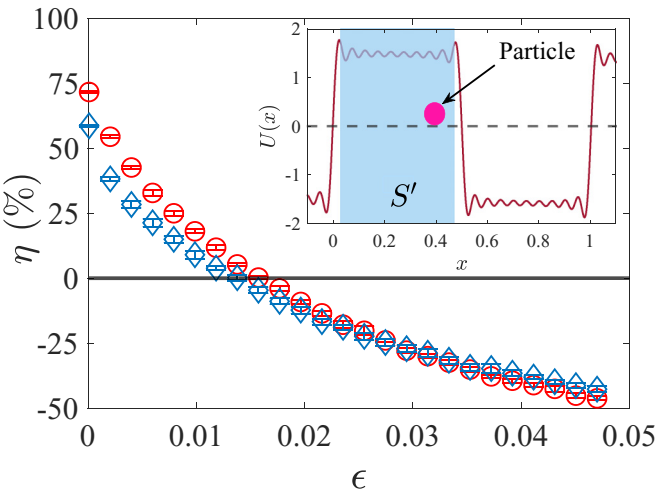

FIG. 9. Comparison of efficiency values with different values of ϵ in the case of square potential. The inset shows the newly defined region (S') of particle's position measurement. S' covers approximately the raised portion of the potential. The red circles correspond to efficiency values when the particle's position is measured in S'. The blue diamonds correspond to efficiency values when the particle's position is measured only in half of the raised portion of the potential. Such a region starts from the middle of the raised portion of the potential at $x = 0.24$ and ends at $x = 0.49$. It is seen that choosing the entire raised portion of the square potential as the measurement region (S') gives better efficiency values comparing to measuring the particle's position only in half of the raised portion of the potential, for all values of ϵ where efficiency is positive. The error bars in the figure are standard deviations.

The region where particle is searched for during measurement is chosen to be the position values where the potential is approximately, U_0 (S' in the figure). This region extends from $x = 0.03$ to $x = 0.47$ for the approximate square potential modelled above. We have also computed the efficiency for the case when the region where particle is searched for is half of the raised portion of the potential. The variation of engine efficiency is shown in Fig. 9. For the smallest feedback delay, switching to square potential has increased the efficiency to almost 71%. Note that for the sinusoidal potential with same U_0 and optimal s is only 54%. Like in the case for sinusoidal potential, the contribution to the numerator of η coming from ΔF is negligible compared to $-\langle W \rangle$.

We have also studied the variation of the efficiency and power as a function of the amplitude of the square potential. The results are shown along with that for the sinusoidal potential (see Figs. 6 and 7). It is seen that the square potential offers better efficiency and work per cycle for almost the entire range of U_0. The maximal work per cycle for the square potential is almost double of that obtained for the sinusoidal potential with $s = 0.25$. The maximum efficiency for the square case is above 90% compared to the 80% for the sinusoidal one.

V. VERIFYING GENERALIZED FLUCTUATION THEOREMS

The GIFT for processes which include an error-free feedback mechanism is given by [40]

$$\langle e^{(\Delta F - W)/k_B T - I + I_u} \rangle = 1, \tag{10}$$

where the average is carried out over multiple trials, all starting off with the initial state of the system in equilibrium at temperature T. The quantity I_u is the unavailable information associated with each measurement outcome. It is determined by running the process backwards without feedback and finding the probability, p_1 (p_2) of finding the particle within region S (outside of region S) if the particle was spotted in S (not spotted in S) in the forward process. I_u is given by $-\log(p_1)$ ($-\log(p_2)$) if the particle is spotted in S (not spotted in S) in the forward process. The generalized form of Jarzynski equality (GJE) when feedback is present can be written as [48]

$$\langle e^{(\Delta F - W)/k_B T} \rangle = \gamma, \tag{11}$$

where $\gamma = p_1 + p_2$. If the process is completely reversible, then $p_1 = p_2 = 1$ and we have the maximum value of $\gamma = 2$. The unavailable information in this case becomes zero. Thus γ measures the efficacy of information to free-energy conversion and its value can vary between 0 and 2 for the present protocol, with two possible measurement outcomes used for the feedback process. One expects to regain the usual JE if there is no correlation between the outcome and the feedback, which is expected to happen when the waiting time ϵ is comparable to the equilibration time. As the feedback procedure becomes more and more irreversible, one should even expect the γ value to drop below 1 due to the very low efficacy of the process.

We verify the GJE in the simulations by averaging over a large number of trials (10^6 runs for each value of ϵ) that is warranted by the exponential average involved [34,49]. We have calculated γ in our simulation as follows: The time-reversed trajectories are obtained by running the process in time-reversed manner with and without potential flip. The reverse cycle starts at $t = 0$ with the system in equilibrium and the potential is flipped at $t = \tau - \epsilon$ (for finding p_1) or not flipped (for finding p_2). At $t = \tau$, a measurement of the particle's position is done. If the potential is flipped in the reverse run, then the probability for finding the particle in region S is calculated, which gives p_1. For a run without potential flip, the probability for finding the particle outside S is calculated, which is p_2. The sum of the two probabilities give us γ. The value of p_1 and p_2 are estimated by averaging over 10^6 cycles each and the error in their estimates is also determined. The average value of p is determined using similar averages in the forward cycle.

Variation of left-hand and right-hand sides of GJE as a function of ϵ for the sinusoidal potential case with $F_d = 0.1$ is shown in Fig. 10. As expected, the value of γ starts above 1 but below the maximum value of 2 for small values of ϵ and is seen to tend toward 1 for large values of ϵ. The difference (in percentage) between the computed right-hand side and left-hand side of the equation is given in Fig. 11(b). The slight discrepancy that exists (less than 1%), as seen from Fig. 11 can be attributed to the fact that with the driving force on, the starting state is not a true equilibrium state. This mismatch is more apparent if the drive is stronger as can be seen from data in Fig. 12 which is for a driving force $F_d = 0.6$ and the corresponding discrepancy in shown in Fig. 11(c). Figure 11(a) shows the difference between right-hand side and left-hand side of GJE for $F_d = 0$. One can see that the difference has reduced and to within the statistical fluctuations

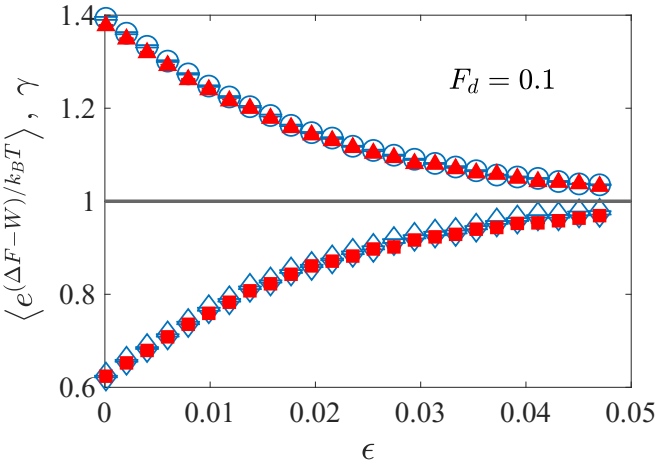

FIG. 10. Variation of left and right-hand side of GJE with feedback delay, ϵ, for a driving force value $F_d = 0.1$. The open circles give the left-hand side of Eq. (11) and the solid triangles the right-hand side. At large values of ϵ the feedback effect becomes minimal and conventional JE is approached. The open diamonds and solid squares too represent the same relation but now for a feedback protocol that is designed to make the process more irreversible. The error bars in the figure are standard deviations.

the GJE is valid for all ϵ values. The verification of GIFT carried out for $F_d = 0, F_d = 0.1$, and $F_d = 0.6$ are shown in Figs. 13(a), 13(b) and 13(c), respectively. The relation is found to hold for all values of ϵ for the zero drive case. We have also verified the GJE for a feedback protocol that leads to values of γ less than 1. This was achieved by altering the feedback protocol such that the flip of the potential is carried out when the particles is *not* spotted in S and the potential is left unaltered when the particle is spotted in S. The data given in Fig. 10 (bottom set) asserts the validity of the GJE for this case.

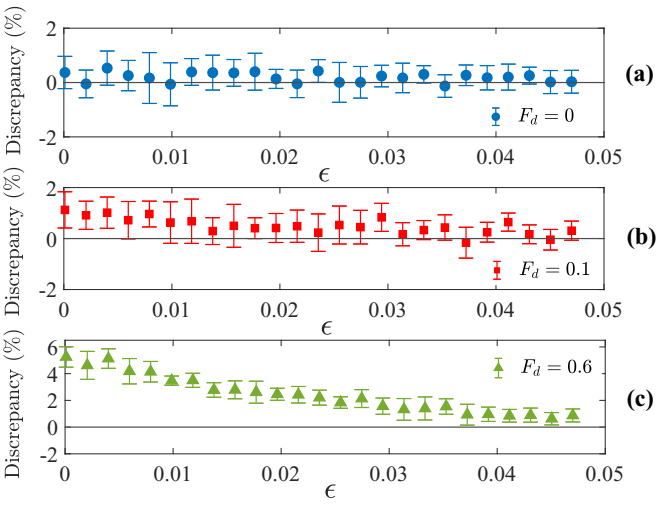

FIG. 11. Discrepancy in percentage between the left- and right-hand sides of GJE for (a) $F_d = 0$, (b) $F_d = 0.1$, and (c) $F_d = 0.6$. The discrepancy is calculated as $[\langle e^{(\Delta F - W)/k_B T} \rangle - \gamma]/\langle e^{(\Delta F - W)/k_B T} \rangle$ in percentage. The error bars in the figure are standard deviations.

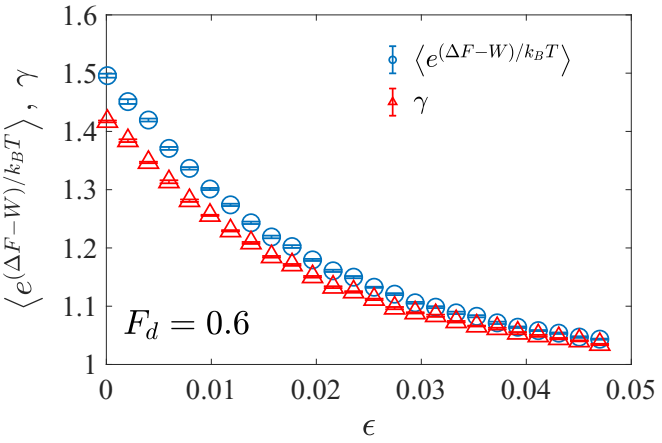

FIG. 12. Verification of GJE for larger driving force, $F_d = 0.6$. The discrepancy between the forward and reverse values are larger as compared to lower driving forces. The error bars in the figure are standard deviations.

VI. CONCLUSION

We have carried out a Brownian dynamics simulation of a driven colloidal particle in one dimensional periodic potential with feedback control. An experimental study of a similar system using feedback control for converting the obtained information about the particle's position to free energy has been conducted before [13]. The control over various model parameters as well as advantage of better averaging in simulations has allowed us to explore the model in great detail. Shorter waiting time for potential flip (in simulations, one can implement an almost instantaneous flip of the potential if the particle is spotted in S) as well as introduction of feedback process when the particle is not observed during measurement allows one to reach an efficiency close to 43%. Optimization carried out by varying both the amplitude of the sinusoidal

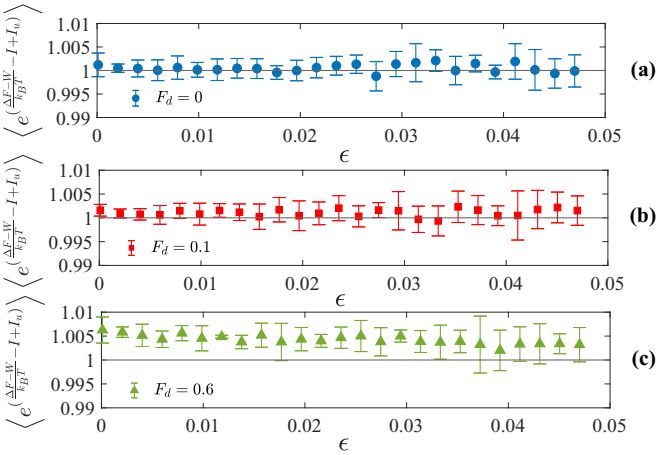

FIG. 13. The verification of generalized integral fluctuation theorem for the case with (a) $F_d = 0$, (b) $F_d = 0.1$, and $F_d = 0.6$. There is a slight improvement of the validity of the relation for small drive. The values are visibly violating the relation for larger value of drive. GIFT is found to be valid for all values of ϵ studied with zero or small drive. The error bars in the figure are standard deviations.

part of the potential U_0 as well as the width of the region S in the model takes the efficiency value to 80%. This is almost the double the value of η before optimization. But this comes at the cost of low value of resultant work extracted per cycle. For comparison, the experimentally obtained efficiency for a similar engine using colloidal particle in sinusoidal potential [13] is 28% and for an experimental implementation of Brownian motor working in a harmonic potential [23] is 35%.

The efficiency at maximum work per cycle that we have obtained is about 40% for the sinusoidal potential. It has to be kept in mind that the optimization has not been exhaustive and better combinations of power and efficiency could be possible. For comparison, the experimentally obtained efficiency at maximum power for the experimental implementation of Brownian motor working in a harmonic potential referred to above [23] is 19%. It is not surprising that with the current model the conversion of all the available information to work is not possible. The fact that we are constraining the potential change after the measurement to the one arising from a flip does not allow one to tune the Hamiltonian post measurement to one where the post measurement distribution is the equilibrium distribution of the new Hamiltonian. This invariably leads to irreversibility in the process with the associated dissipation [30].

We have been able to work around the above limitation to an extent by using a square potential instead of the sinusoidal one. For large amplitude of the square potential, the flipping of the potential during the feedback process leads to a new Hamiltonian whose equilibrium distribution closely matches with the nonequilibrium distribution resulting from the measurement process. We find that both the work done per cycle as well as the efficiency has much better values for this choice. The efficiency goes above 90% for high values of amplitude and the efficiency at maximum work per cycle is 53%. This suggests that using appropriate potential shape can lead to an appreciable change in the performance of this type of information engine based on a particle moving in a periodic potential.

We have numerically verified GJE as well as GIFT for different values of feedback delay. The left and right-hand sides of the GJE [see Eq. (11)] have been found independently using the forward and time-reversed process respectively. We find that for zero drive force, fluctuation theorems are valid to within the simulation accuracy. The GJE for a similar system was verified experimentally [13] and found to hold with 3% discrepancy. The error margin in the present simulation results are smaller with error bars down to less than 1%. We observe, like in the experiment, that for larger drives, the deviations in GJE is violated by a larger margin (around 5% for $F_d = 0.6$). This is expected since the condition of the starting state being an equilibrium one is then not met with [38,48]. Further, we have also verified GJE for the case when efficacy is a value less than 1, implemented by changing the feedback process. It is found that for zero drive, the GIFT is valid for the waiting times studied. Though GIFT has been experimentally verified for and theoretically checked in information engine models based on a particle moving in a harmonic potential [16,40], this is the first time it is being verified for an error free information engine based on a particle moving in a periodic potential with feedback process based on potential flips.

All the feedback studies we have carried out in this work are based on single cycle processes. The study can be extended by exploring the effects of correlation on efficiency of such an information engine by simulating multicycle realizations. There are preliminary indications that multicycle processes can lead to higher efficiencies. Experimental implementation of the information engine based on a colloidal particle moving in a square potential should be possible.

ACKNOWLEDGMENT

The authors acknowledge P. N. Deepak for fruitful discussions and careful reading of the manuscript. T.J. would like to acknowledge Science and Engineering Research Board (SERB), India for financial support (Project No. CRG/2020/003646).

[1] J. Clerk Maxwell, *Theory of Heat* (Longmans, Green, & Co., London, UK, 1871).
[2] K. Maruyama, F. Nori, and V. Vedral, Rev. Mod. Phys. **81**, 1 (2009).
[3] L. Szilard, Behav. Sci. **9**, 301 (1964).
[4] J. Earman and J. D. Norton, Stud. Hist. Philos. Sci. B: Stud. Hist. Philos. Mod. Phys. **29**, 435 (1998).
[5] J. Earman and J. D. Norton, Stud. Hist. Philos. Sci. B: Stud. Hist. Philos. Mod. Phys. **30**, 1 (1999).
[6] M. Hemmo and O. Shenker, J. Philosophy **107**, 389 (2010).
[7] J. D. Norton, Stud. Hist. Philos. Sci. B: Stud. Hist. Philos. Mod. Phys. **42**, 184 (2011).
[8] L. B. Kish and C. G. Granqvist, Europhys. Lett. **98**, 68001 (2012).
[9] R. Landauer, IBM J. Res. Dev. **5**, 183 (1961).
[10] C. H. Bennett, Int. J. Theor. Phys. **21**, 905 (1982).
[11] T. Sagawa and M. Ueda, Phys. Rev. Lett. **102**, 250602 (2009).
[12] *Mawell's Demon 2: Entropy, Classical and Quantum Information, Computing*, edited by H. S. Leff and A. F. Rex (Institute of Physics Publishing, Bristol and Philadelphia, 2003).
[13] S. Toyabe, T. Sagawa, M. Ueda, E. Muneyuki, and M. Sano, Nat. Phys. **6**, 988 (2010).
[14] A. Bérut, A. Arakelyan, A. Petrosyan, S. Ciliberto, R. Dillenschneider, and E. Lutz, Nature **483**, 187 (2012).
[15] T. K. Saha, J. N. E. Lucero, J. Ehrich, D. A. Sivak, and J. Bechhoefer, Proc. Natl. Acad. Sci. USA **118**, e2023356118 (2021).
[16] G. Paneru, D. Y. Lee, T. Tlusty, and H. K. Pak, Phys. Rev. Lett. **120**, 020601 (2018).
[17] J. V. Koski, V. F. Maisi, J. P. Pekola, and D. V. Averin, Proc. Natl. Acad. Sci. USA **111**, 13786 (2014).
[18] B.-L. Najera-Santos, P. A. Camati, V. Métillon, M. Brune, J.-M. Raimond, A. Auffèves, and I. Dotsenko, Phys. Rev. Res. **2**, 032025(R) (2020).

[19] D. V. Averin, M. Möttönen, and J. P. Pekola, Phys. Rev. B **84**, 245448 (2011).
[20] P. A. Camati, J. P. S. Peterson, T. B. Batalhão, K. Micadei, A. M. Souza, R. S. Sarthour, I. S. Oliveira, and R. M. Serra, Phys. Rev. Lett. **117**, 240502 (2016).
[21] M. Naghiloo, J. J. Alonso, A. Romito, E. Lutz, and K. W. Murch, Phys. Rev. Lett. **121**, 030604 (2018).
[22] K. Chida, S. Desai, K. Nishiguchi, and A. Fujiwara, Nat. Commun. **8**, 15310 (2017).
[23] G. Paneru, D. Y. Lee, J.-M. Park, J. T. Park, J. D. Noh, and H. K. Pak, Phys. Rev. E **98**, 052119 (2018).
[24] M. Rico-Pasto, R. K. Schmitt, M. Ribezzi-Crivellari, J. M. R. Parrondo, H. Linke, J. Johansson, and F. Ritort, Phys. Rev. X **11**, 031052 (2021).
[25] J. N. E. Lucero, J. Ehrich, J. Bechhoefer, and D. A. Sivak, Phys. Rev. E **104**, 044122 (2021).
[26] L. Dinis and J. M. R. Parrondo, Entropy **23**, 8 (2020).
[27] P. S. Pal, S. Rana, A. Saha, and A. M. Jayannavar, Phys. Rev. E **90**, 022143 (2014).
[28] D. Abreu and U. Seifert, Europhys. Lett. **94**, 10001 (2011).
[29] M. Bauer, D. Abreu, and U. Seifert, J. Phys. A: Math. Theor. **45**, 162001 (2012).
[30] J. M. Parrondo, J. M. Horowitz, and T. Sagawa, Nat. Phys. **11**, 131 (2015).
[31] H.-H. Hasegawa, J. Ishikawa, K. Takara, and D. Driebe, Phys. Lett. A **374**, 1001 (2010).
[32] M. Esposito and C. Van den Broeck, Europhys. Lett. **95**, 40004 (2011).
[33] J. M. Horowitz and J. M. Parrondo, New J. Phys. **13**, 123019 (2011).
[34] C. Jarzynski, Annu. Rev. Condens. Matter Phys. **2**, 329 (2011).
[35] U. Seifert, Rep. Prog. Phys. **75**, 126001 (2012).
[36] D. J. Evans, E. G. D. Cohen, and G. P. Morriss, Phys. Rev. Lett. **71**, 2401 (1993).
[37] G. Gallavotti and E. G. D. Cohen, Phys. Rev. Lett. **74**, 2694 (1995).
[38] C. Jarzynski, Phys. Rev. Lett. **78**, 2690 (1997).
[39] G. E. Crooks, Phys. Rev. E **60**, 2721 (1999).
[40] Y. Ashida, K. Funo, Y. Murashita, and M. Ueda, Phys. Rev. E **90**, 052125 (2014).
[41] J. V. Koski, V. F. Maisi, T. Sagawa, and J. P. Pekola, Phys. Rev. Lett. **113**, 030601 (2014).
[42] G. Paneru, S. Dutta, T. Sagawa, T. Tlusty, and H. K. Pak, Nat. Commun. **11**, 1012 (2020).
[43] G. Paneru and H. K. Pak, Adv. Phys. X **5**, 1823880 (2020).
[44] D. L. Ermak, J. Chem. Phys. **62**, 4197 (1975).
[45] R. L. Stratonovich, Radiotekh. Elektron. **3**, 497 (1958).
[46] P. Reimann, C. Van den Broeck, H. Linke, P. Hänggi, J. M. Rubi, and A. Pérez-Madrid, Phys. Rev. Lett. **87**, 010602 (2001).
[47] C. E. Shannon, Bell Syst. Tech. J. **27**, 379 (1948).
[48] T. Sagawa and M. Ueda, Phys. Rev. Lett. **104**, 090602 (2010).
[49] J. Liphardt, S. Dumont, S. B. Smith, I. Tinoco Jr, and C. Bustamante, Science **296**, 1832 (2002).